IJIRSET
International Journal of Innovative Research in Science | Engineering | Technology

ISSN(O): 2319-8753
ISSN(P): 2347-6710



International Journal of Innovative Research in Science Engineering and Technology (IJIRSET)

(A Monthly, Peer Reviewed, Refereed, Scholarly Indexed, Open Access Journal)



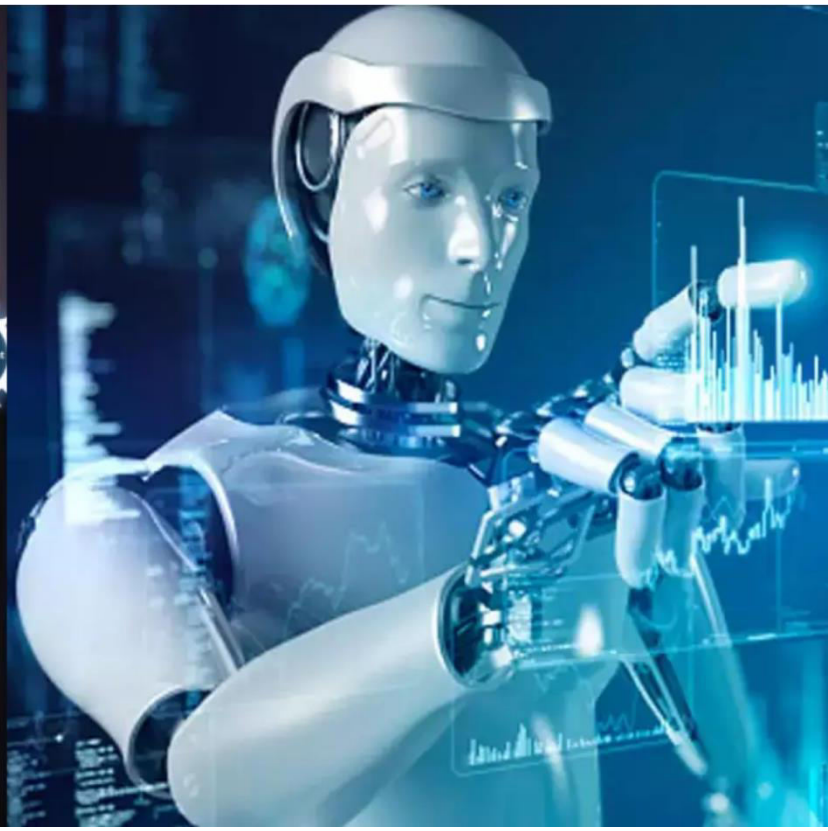

Impact Factor: 9.935

Volume 15, Issue 11, November 2026

International Journal of Innovative Research of Science, Engineering and Technology (IJIRSET)

Impact Factor 9.935

|www.ijirset.com |A Monthly, Peer Reviewed & Refereed Journal| e-ISSN: 2319-8753| p-ISSN: 2347-6710|

Volume 15, Issue 11, November 2026

|DOI: 10.15680/IJIRSET.2026.1511028|

Statistical Modeling of Multivariate EEG Time-Series Data for Multi-Class Stress Classification Using Ensemble Learning

C Sumangali

Lecturer, Dept. of Statistics, NSPR government Degree College for women, hindupur, AP, India-515201

ABSTRACT: Stress is a prevalent global health concern traditionally assessed through subjective psychological evaluations, creating a need for objective, quantifiable physiological measurement. This study presents a comprehensive statistical evaluation of time-series electroencephalographic (EEG) data for the multi-class detection of acute stress. Experimental data was collected from 30 participants who were subjected to a controlled sequence of stress-inducing stimuli, with physiological responses recorded continuously. To transform the longitudinal biosignals into a structured tabular format, we evaluated distinct feature extraction paradigms, specifically contrasting foundational statistical measures of central tendency and dispersion (mean and standard deviation) across 19 EEG channels against traditional frequency-domain characteristics. To assess predictive variance and classification accuracy, four distinct modeling frameworks were utilized: an ensemble gradient-boosting method (LightGBM), K-Nearest Neighbors (KNN), Support Vector Machines (SVM), and Convolutional Neural Networks (CNN). The comparative statistical analysis reveals that the simplified time-domain features (mean and standard deviation) consistently yielded the highest classification accuracy (86.24%), significantly outperforming more complex frequency-band features. Among the evaluated algorithms, the tree-based ensemble method (LightGBM) demonstrated superior predictive stability and accuracy across all test scenarios. Furthermore, time-complexity analysis confirmed the efficiency of this statistical approach, with time-domain feature extraction requiring nearly half the processing time (588 ms) compared to frequency extraction (1,123 ms). An analysis of spatial feature importance further identified specific temporal and frontal electrodes (T8, Fp1, Fz, and C3) as the most statistically significant contributors to stress variance. Finally, integrating the EEG data with concurrent Electrocardiogram (ECG) and Electrodermal Activity (EDA) signals maximized the ensemble model's predictive accuracy to 91.44%. These findings demonstrate that leveraging fundamental statistical features from EEG signals provides a robust, computationally efficient, and highly accurate framework for real-time stress classification, with direct applications in the design of wearable biostatistical monitoring systems.

KEYWORDS: Time-Series Analysis, Ensemble Statistical Learning, Multivariate Classification, Feature Variance, Predictive Modeling, Biostatistics, High-Dimensional Data, Statistical Inference.

I. INTRODUCTION

Stress is an inherent physiological and psychological response to environmental challenges and internal cognitive processes [1], [2]. When this response becomes chronic and remains undetected, it can precipitate severe psychological disorders and long-term mental health degradation [3]. Historically, the evaluation of stress has relied heavily on qualitative psychological methodologies and self-reported questionnaires, which often introduce subjective bias and statistical noise into the data [4], [5]. Recent methodological advancements strongly advocate for the use of objective physiological indicators to establish more robust, empirically verifiable metrics for assessment [4], [5]. Traditional manual examinations by healthcare professionals are often expensive and time-consuming, limiting the scale of data collection [4]. Consequently, developing automated, data-driven statistical models based on continuous physiological time-series data offers a scalable alternative, reducing the analytical burden on both patients and healthcare infrastructure.

Among the diverse array of physiological variables available for analysis, electroencephalography (EEG) time-series data stands out for its capacity to provide a direct, continuous measure of neural variance during stress-inducing conditions [6]. While other peripheral autonomic markers such as the electrocardiogram (ECG) [7], electrodermal activity (EDA) [8], and respiration rate (RSP) [9] demonstrate statistically significant correlations with physiological

International Journal of Innovative Research of Science, Engineering and Technology (IJIRSET)

Impact Factor 9.935

|www.ijirset.com |A Monthly, Peer Reviewed & Refereed Journal| e-ISSN: 2319-8753| p-ISSN: 2347-6710|

Volume 15, Issue 11, November 2026

|DOI: 10.15680/IJIRSET.2026.1511028|

arousal, EEG captures the underlying electrical distributions associated with complex cognitive and emotional shifts [10]. This makes EEG a uniquely high-dimensional dataset, offering profound insights into the complex, multivariate dynamics of the neural stress response that peripheral sensors cannot independently capture [10].

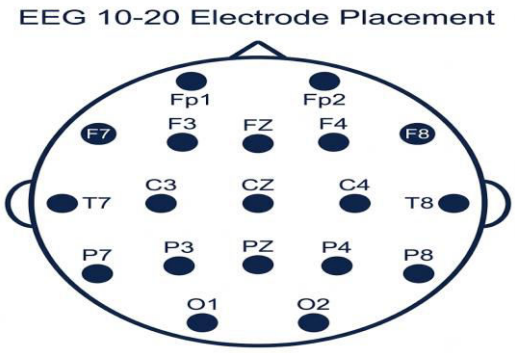

Fig 1: EEG electrodes placement position diagram

The application of statistical learning and classification algorithms to biosignal data allows for the empirical categorization of latent stress states. For example, Heyat et al. [11] employed a suite of probabilistic and ensemble classifiers including Decision Trees (DT), Naive Bayes (NB), Random Forest (RF), and Logistic Regression (LR) to differentiate between stress and non-stress conditions based on average heart rate and RR interval features extracted from ECG data. Similarly, Hosseini et al. [12] modeled stress using normalized EDA signals, applying AdaBoost, RF, and Support Vector Machines (SVM) to establish decision boundaries. Furthermore, Asif et al. [13] investigated human stress classification using EEG signals in response to auditory stimuli, employing sequential minimal optimization, stochastic gradient descent, LR, and Multilayer Perceptron (MLP) architectures to categorize variance into two and three discrete stress classes.

However, the direct ingestion of raw biosignal data into predictive models is statistically suboptimal without rigorous preliminary signal processing [14]. Biosignals are inherently noisy time-series data sampled at a specific frequency, requiring robust cleaning phases prior to analysis. A standard practice to mitigate the curse of dimensionality is to reduce the raw data into a lower-dimensional feature space. For EEG analysis, this typically involves extracting parameters across various domains: the time domain (utilizing principal component analysis or independent component analysis), the frequency domain (deriving power spectral density (PSD) via Fourier transforms), and the time-frequency domain (using wavelet analysis) [15]. Despite the computational benefits of dimensionality reduction in later modeling stages, optimal feature selection remains a persistent statistical challenge [10]. PSD interpretation requires substantial domain expertise, and wavelet analysis is highly sensitive to the a priori selection of the basis function. Furthermore, the extraction of these complex transformations introduces significant computational overhead, which can limit their utility in real-time, resource-constrained inference applications.

Recent advancements in sensor technology have facilitated the continuous collection of physiological data outside controlled clinical environments, providing vast empirical datasets for longitudinal stress analysis. Simple, consumer-grade EEG devices that operate without conductive gels offer an accessible means of data collection [16]. However, these devices typically capture a limited number of variables. A critical statistical inquiry is whether the variance captured by an isolated EEG sensor provides sufficient explanatory power for accurate stress classification, or if it must be supplemented with peripheral multimodal data, such as EDA and ECG from wristbands, to reduce predictive error. Most existing literature focuses heavily on maximizing the performance metrics of machine learning algorithms while neglecting to isolate and quantify the specific statistical contribution of EEG data relative to other biosignals.

International Journal of Innovative Research of Science, Engineering and Technology (IJIRSET)

Impact Factor 9.935

|www.ijirset.com |A Monthly, Peer Reviewed & Refereed Journal| e-ISSN: 2319-8753| p-ISSN: 2347-6710|

Volume 15, Issue 11, November 2026

|DOI: 10.15680/IJIRSET.2026.1511028|

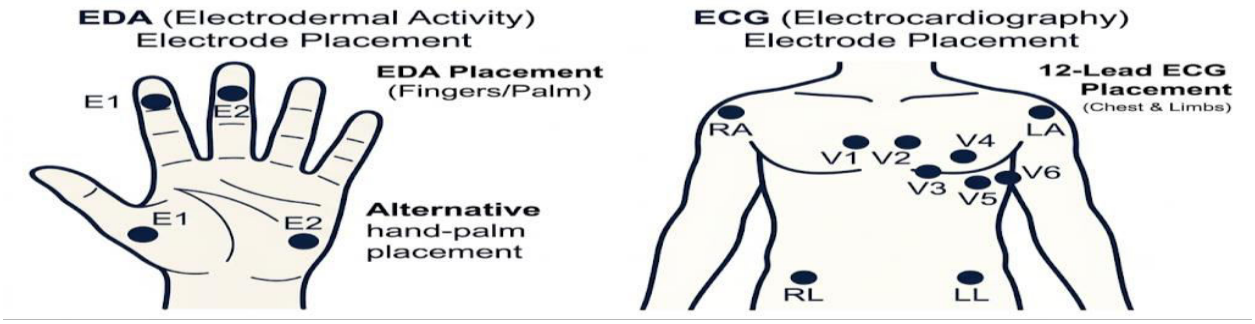

Fig 2: EDA and ECG electrodes placement position diagram

In this context, our study serves as a critical bridge, designed to empirically evaluate the statistical contribution and predictive weight of EEG data in multi-class stress detection compared to established autonomic measures like ECG and EDA. Furthermore, we conduct a channel-specific variance analysis to determine which spatial EEG electrodes provide the most statistically significant data, thereby informing the optimized design of future, less intrusive wearable monitors. As a secondary methodological contribution, we explore alternative feature extraction paradigms, demonstrating that simple, low-computational time-domain statistics specifically the mean and standard deviation retain sufficient discriminative variance to achieve high classification accuracy.

II. RELATED WORK

Recent literature has explored various statistical and computational methodologies utilizing biosignals, primarily EEG, for stress classification. Samarpita et al. [17] trained diverse ensemble and non-parametric models such as Random Forest (RF), K-Nearest Neighbors (KNN), and XGBoost but limited their statistical power to a small sample of 4 subjects and 4 channels. Baliga et al. [18] utilized alpha and beta frequency bands across 40 subjects, but the temporal data collection was restricted to 80-second intervals. Marthinsen et al. [19] applied a Genetic Algorithm for channel selection and Wavelet Scattering for feature extraction across 8 channels prior to fitting Support Vector Machine (SVM) and Convolutional Neural Network (CNN) models. In contrast, our study captures a substantially richer multivariate feature space by recording 19 continuous channels over approximately 22 minutes across 30 participants, thereby significantly enhancing both the spatial and temporal resolution of the dataset.

Other studies have relied heavily on complex mathematical transformations to extract variance from the data. Alshorman et al. [20] applied Fast Fourier Transforms (FFT) to measure power density across five frequency bands before fitting probabilistic and max-margin classifiers (Naive Bayes and SVM). Similarly, Nirabi et al. [21] utilized Discrete Wavelet Transforms (DWT) for feature extraction across 7 channels. Unlike these approaches, which depend on computationally heavy frequency-domain transformations, our work investigates the predictive efficacy of fundamental time-domain statistical moments specifically, the mean and standard deviation. This approach aims to capture the necessary variance without introducing the high computational overhead associated with FFT or DWT.

Several investigations have combined multiple physiological signals to increase model accuracy, often resulting in varying degrees of feature dimensionality. Hemakom et al. [22] extracted a high-dimensional feature space (147 variables) from just 8 EEG channels combined with ECG data. Conversely, Zontone et al. [23] and Affani [24] modeled stress using highly restricted feature sets (9 and 5 variables, respectively) derived strictly from EDA and ECG signals without EEG. While expanding the feature space as seen in [22] can theoretically capture more information, it significantly increases the risk of multicollinearity, the inclusion of redundant variables, and subsequent model overfitting. High dimensionality also inflates computation time and complicates feature selection. Our methodology balances this statistical trade-off by utilizing a carefully selected set of 38 features, avoiding the statistical penalties of both extreme high-dimensionality and under-parameterization.

Expanding beyond strictly physiological data, some researchers have incorporated behavioral and environmental covariates into their models. Umematsu et al. [25] utilized a massive multimodal feature set (375 variables) encompassing EDA, mobile phone usage, location data, and behavioral surveys to forecast stress levels. Bobade and

International Journal of Innovative Research of Science, Engineering and Technology (IJIRSET)

Impact Factor 9.935

|www.ijirset.com |A Monthly, Peer Reviewed & Refereed Journal| e-ISSN: 2319-8753| p-ISSN: 2347-6710|

Volume 15, Issue 11, November 2026

|DOI: 10.15680/IJIRSET.2026.1511028|

Vani [26] similarly integrated 39 features from a diverse array of motion and physiological sensors (e.g., acceleration, blood volume pulse, body temperature, electromyogram, and EDA). While multimodal integration is valuable, it introduces complex confounding effects and requires sophisticated methods to align asynchronous data sources. Our study deliberately isolates EEG data to quantitatively evaluate its specific statistical contribution relative to baseline cardiovascular and electrodermal metrics (ECG and EDA), thereby streamlining the variance analysis and avoiding the complexities of multimodal integration.

Finally, a prevalent gap in the reviewed literature is the absence of spatial feature importance analysis for EEG data. Unlike previous studies, this work conducts a rigorous channel importance analysis to statistically quantify which specific spatial locations (electrodes) contribute the most variance to the stress classification task. This dimensional reduction technique paves the way for designing optimized, data-efficient wearable sensors by reducing the required number of electrodes. Furthermore, our review indicates an underutilization of LightGBM a highly efficient gradient-boosting framework capable of handling tabular distributions with greater speed despite its proven potential to outperform traditional predictive models in large datasets.

III. METHODS

The fundamental analytical framework of the proposed stress recognition system is illustrated in Fig. 3. The primary objective is to evaluate the specific statistical contribution of electroencephalography (EEG) time-series data in multi-class stress detection. To achieve this, two parallel data streams were established: one processing multivariate continuous EEG signals, and the second handling autonomic cardiovascular (ECG) and electrodermal (EDA) signals. Gathering all bio signals simultaneously from the same subject under an identical experimental protocol ensures paired-sample consistency for comparative statistical evaluation.

The raw data was initially subjected to filtering and artifact removal procedures to minimize observational noise. Subsequently, feature extraction methods were implemented to transform the longitudinal, non-stationary time series into a structured tabular matrix suitable for multivariate statistical modeling. Discrete categorical labels (stress, neutral, and relax) were derived through empirical inspection and validated against behavioral measures, followed by class balancing to correct for distribution skewness. Finally, multiple supervised learning algorithms spanning diverse functional complexities were fitted and evaluated.

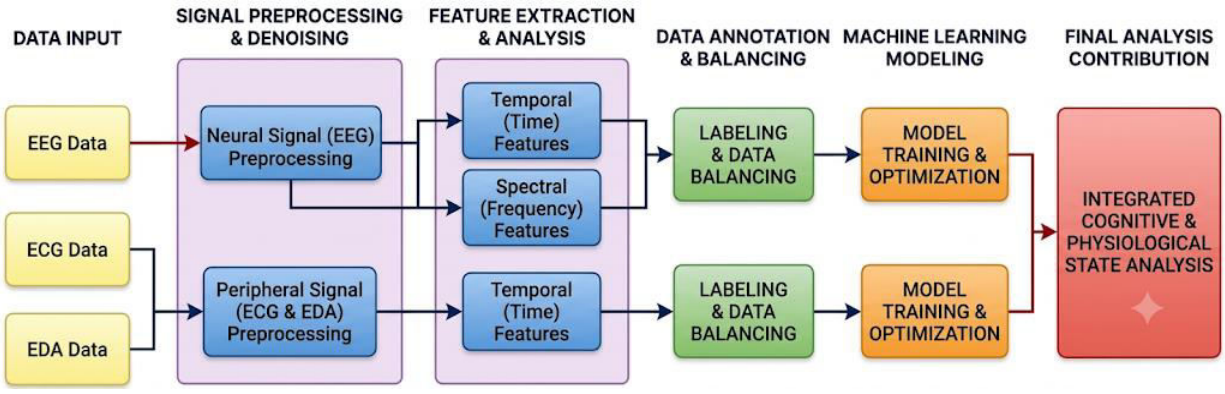

Fig 3: Proposed methodology diagram for Emotion Recognition

3.1 Data Collection Protocol

A cohort of 30 healthy student participants was recruited for this study ($N = 30$), consisting of an equal distribution of 15 males and 15 females. The age distribution of the sample ranged from 18 to 38 years, with a sample mean (μ) of 20.8 years and a standard deviation (σ) of 3.4 years. Balanced gender stratification was deliberately adopted as an experimental control to mitigate potential confounding variance driven by sex-differentiated physiological and emotional response patterns. The experimental protocol received formal approval from the institutional ethical committee, ensuring strict compliance with all standard regulatory codes (CEISH-UPV/EHU, BOPV 32 (M10 2016 189)).

International Journal of Innovative Research of Science, Engineering and Technology (IJIRSET)

Impact Factor 9.935

|www.ijirset.com |A Monthly, Peer Reviewed & Refereed Journal| e-ISSN: 2319-8753| p-ISSN: 2347-6710|

Volume 15, Issue 11, November 2026

|DOI: 10.15680/IJIRSET.2026.1511028|

3.2 Devices and Instrumentation

Continuous physiological measurements were collected using two synchronized recording systems:

- **EEG Acquisition:** Neural activity was captured using the Enobio system (Neuroelectrics) configured with 19 scalp electrodes placed in accordance with the international 10–20 standard positioning framework (Fig. 1). Continuous temporal data was recorded via NIC2 software at a uniform sampling frequency of 500 Hz.
- **ECG and EDA Acquisition:** Peripheral autonomic markers were acquired using BIOPAC MP36 hardware (Biopac Systems Inc., USA) and recorded via the BIOPAC Student Lab platform. Channel 1 recorded the continuous ECG using standard thoracic electrode placements (Fig. 2), while Channel 2 captured the continuous EDA using skin-conductance sensors placed on two fingers of the non-dominant hand (Fig. 2). The sampling rate across all peripheral channels was uniformly synchronized at 500 Hz.

3.3 Experimental Stress Induction Protocol

The experimental procedure was adapted from the controlled stress-induction methodology proposed by Martínez et al. [5]. While prior protocols often relied on a single continuous activity which failed to account for heterogeneous intra-individual and inter-individual response variance this study utilized an alternating multi-task paradigm designed to stimulate diverse cognitive stressors. The experimental timeline incorporated three active stress-induction stages separated by baseline recovery intervals during which participants watched two-minute calming audiovisual sequences (Fig. 4):

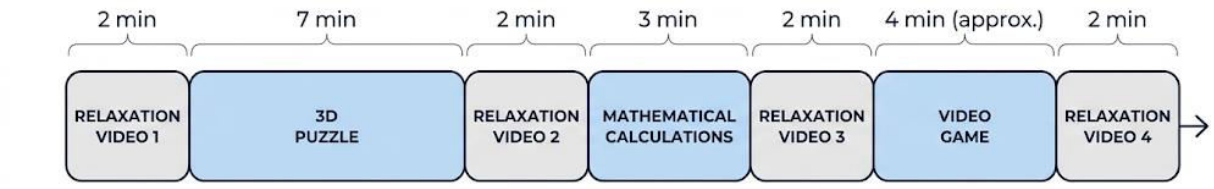

Fig 4: Test Sequence of signal time line

3.3.1 3D Geometric Puzzle: Participants were allotted a maximum duration of 7 minutes to construct a complex three-dimensional puzzle. At the 5-minute mark, an explicit verbal time-constraint cue was introduced to induce performance-related psychological arousal. Following the task, subjects were presented with the printed analytical solution; the discrepancy between physical manipulation and paper-based conceptualization served as an additional source of cognitive frustration.

3.3.2 Adaptive Mental Arithmetic: Sequential mental calculations of increasing computational difficulty were administered for a fixed duration of 3 minutes. Upon delivering a correct response, the subject was immediately presented with a more demanding arithmetic problem under time pressure, establishing a continuous state of cognitive demand [28], [29].

3.3.3 Adaptive Mobile Gaming: Participants completed a high-tempo mobile music-coordination game where difficulty scaled dynamically based on player competence, ensuring consistent mental load and engagement.

Following the active testing sequences, qualitative validation data was collected via structured interviews and an abbreviated self-assessment manikin (SAM) questionnaire [40]. This allowed self-reported psychological states to be cross-referenced with the continuous biosignal measurements.

3.4 Signal Preprocessing and Artifact Filtering

Rigorous signal conditioning was applied to isolate clean neural dynamics from non-cerebral noise (Fig. 5) [30]:

International Journal of Innovative Research of Science, Engineering and Technology (IJIRSET)

Impact Factor 9.935

|www.ijirset.com |A Monthly, Peer Reviewed & Refereed Journal| e-ISSN: 2319-8753| p-ISSN: 2347-6710|

Volume 15, Issue 11, November 2026

|DOI: 10.15680/IJIRSET.2026.1511028|

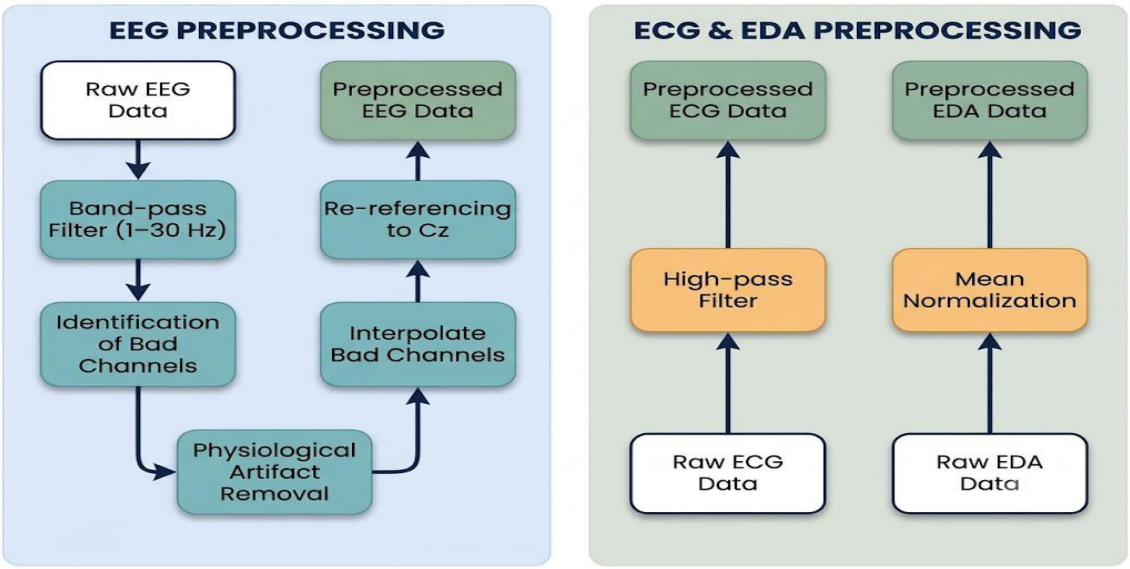

Fig. 5: EEG, ECG and EDA Signal Processing Procedure

3.4.1 EEG Preprocessing: The continuous EEG signals were band-pass filtered between 0.1 Hz and 45 Hz to eliminate low-frequency drift and high-frequency power-line noise. Channels displaying abnormal impedance or severe persistent contamination were identified as defective. To maintain a uniform, high-dimensional coordinate space ($19 \times N$) across all subjects without data truncation, defective channels were reconstructed using spherical spline interpolation rather than absolute deletion [32]. Ocular, cardiac, and myogenic artifacts were isolated and removed using Independent Component Analysis (ICA), which performs linear decomposition to minimize mutual statistical dependence among component sources [31]. Finally, to standardize potential across the spatial array, data was computationally re-referenced from the initial ground reference to the central vertex electrode (C_z).

3.4.2 ECG and EDA Preprocessing: ECG signals were treated with a digital high-pass filter to eliminate baseline wander and movement artifacts. To account for inter-individual differences in baseline perspiration and local ambient laboratory conditions, EDA signals were processed using standard mean-normalization.

3.5 Feature Extraction and Dimensionality Transformation

To map the longitudinal time-series vectors into an empirical feature space, continuous signals were segmented into discrete, non-overlapping temporal windows.

3.5.1 EEG Feature Sets: With a recording duration of approximately 22 minutes at 500 Hz, segments of 500 samples were delineated to represent 1-second epochs, where each epoch serves as an independent observational unit. Two primary statistical paradigms were extracted:

3.5.1.1 Time-Domain Statistical Moments: The sample mean (μ) and standard deviation (σ) were computed for each temporal window across all 19 channels, yielding a compact 38-dimensional feature vector. For a given discrete time-series window consisting of N samples ($N = 500$ for 1-second epochs at 500 Hz), the sample mean is defined as the central tendency of the signal amplitude:

$$\mu = \frac{1}{N}\sum_{i=1}^{N} x_i \qquad \ldots.(1)$$

International Journal of Innovative Research of Science, Engineering and Technology (IJIRSET)

Impact Factor 9.935

|www.ijirset.com |A Monthly, Peer Reviewed & Refereed Journal| e-ISSN: 2319-8753| p-ISSN: 2347-6710|

Volume 15, Issue 11, November 2026

|DOI: 10.15680/IJIRSET.2026.1511028|

The standard deviation reflects the amplitude dispersion and temporal voltage fluctuations, computed as:

$$\sigma = \sqrt{\frac{1}{N-1}\sum_{i=1}^{N}(x_i - \mu)^2} \qquad \ldots.(2)$$

These fundamental moments provide high descriptive utility at minimal computational cost.

3.5.1.2 Frequency-Domain Spectral Measures: The continuous frequency spectrum was segmented into five standard neurological bands: Delta (0.5–4 Hz), Theta (4–8 Hz), Alpha (8–14 Hz), Beta (14–30 Hz), and Gamma (30–45 Hz) [33]. Power Spectral Density (PSD) was computed for each band across all electrodes to quantify power distribution across oscillatory bands [34], [35].

3.5.1.3 Combined Representation: A concatenated feature vector merging time-domain moments and spectral density parameters ("Mean & std + bands").

3.6 ECG and EDA Feature Sets: Because a complete human cardiac cycle averages 0.8 seconds [36], a 1-second window is insufficient for periodic cardiovascular analysis. Consequently, a 10-second window length was established for ECG and aligned with EDA signals to capture stable autonomic shifts [37], [38]. The first-order moments (μ and σ) were computed over these intervals to maintain methodological consistency with the EEG domain.

3.7 Empirical Labeling and Class Balancing

A three-class categorical scheme was established: Stress, Relax, and Neutral. The Neutral class was introduced to capture transitional and ambiguous intervals, preventing forced classification of indistinct affective states. Supervised ground-truth labels were generated through empirical visual inspection of the concurrent autonomic time series (Fig. 6). Specifically, marked decreases in EDA alongside stable ECG intervals denoted parasympathetic dominance (Relax), whereas pronounced increases in EDA accompanied by ECG variability signaled sympathetic activation (Stress) [39]. These temporal markers were cross-validated using the subjective SAM ratings and applied identically across the synchronized EEG windows.

To resolve empirical class frequency imbalances that introduce majority-class prediction bias [41], random oversampling was implemented on minority-class samples. Synthetic interpolation techniques like SMOTE [42] were avoided because they assume local linear configurations between instances an assumption that often fails when applied to the complex non-linear manifolds of continuous neural dynamics, risking the introduction of synthetic noise.

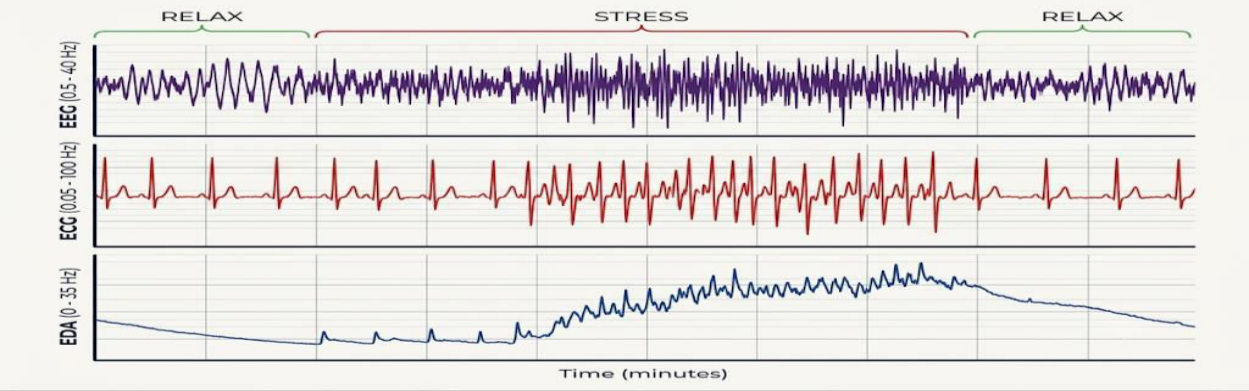

Fig. 6: EEG, ECG and EDA Signal Lebling Procedure

3.8 Predictive Modeling Frameworks

Four supervised classification algorithms spanning parametric, non-parametric, and deep representation architectures were selected:

International Journal of Innovative Research of Science, Engineering and Technology (IJIRSET)

Impact Factor 9.935

|www.ijirset.com |A Monthly, Peer Reviewed & Refereed Journal| e-ISSN: 2319-8753| p-ISSN: 2347-6710|

Volume 15, Issue 11, November 2026

|DOI: 10.15680/IJIRSET.2026.1511028|

3.8.1 LightGBM: A gradient-boosting decision tree framework optimized for tabular data that constructs ensembles through leaf-wise loss reduction, offering high computational speed and effective handling of non-linear interactions [43], [44].

The algorithm additively minimizes the objective loss function $\mathcal{L}$ over iterations t:

$$\mathrm{Obj}^{(t)} = \sum_{i=1}^{n} \mathcal{L}\left(y_i, \hat{y}_i^{(t-1)} + f_t(x_i)\right) + \Omega(f_t) \qquad \ldots.(3)$$

where $\Omega(f_t)$ is the regularization term penalizing model complexity. This approach offers high computational speed and effective handling of complex non-linear autonomic interactions.

3.8.2 Support Vector Machine (SVM): A maximum-margin classifier fitted with a non-linear Radial Basis Function (RBF) kernel to map input vectors into higher-dimensional reproducing kernel Hilbert spaces [46]. The RBF kernel computes the similarity between two feature vectors x and x' as:

$$K(x, x') = \exp\left(-\frac{||x - x'||^2}{2\sigma^2}\right) \qquad \ldots.(4)$$

accommodating the highly non-linear decision boundaries inherent in biosignal data.

3.8.3 K-Nearest Neighbors (KNN): An instance-based non-parametric classifier utilizing tuned Euclidean distance metrics optimized via grid-search cross-validation.

3.8.4 Convolutional Neural Network (CNN): A 16-layer deep neural network designed to capture hierarchical feature representations from input vectors [45].

3.9 Experimental Design and Validation Metrics

The experimental evaluation was structured across five statistical analyses:

- Feature Space Comparative Evaluation: Benchmarking classification accuracy across the three defined EEG feature sets ("Mean & std", "Frequency bands", and combined).
- Temporal Window Sensitivity Analysis: Evaluating parameter stability across 1-second, 10-second, and 20-second temporal windows using LightGBM.
- Intra-Subject vs. Inter-Subject Generalizability: Measuring the variance in classification performance across individual models relative to pooled population models.
- Multivariate Biosignal Contribution: Evaluating incremental predictive gains achieved by combining EEG with peripheral ECG and EDA time series.
- Spatial Electrode Importance Analysis: Quantifying the statistical contribution of individual electrodes using normalized split and gain importance scores within the LightGBM ensemble.

Model evaluation followed an 80/20 train-test split combined with a 5-fold cross-validation scheme to prevent data leakage and provide unbiased parameter estimates. For inter-subject validation, strict subject partitioning was enforced to ensure cross-individual generalizability. Classification performance was evaluated using standard statistical criteria: Accuracy (Acc), Precision (Prec), and the balanced F_1-score.

IV. RESULTS

4.1 Statistical Evaluation of EEG Feature Sets for Stress Detection Table 1 presents the comparative classification accuracies across the varying feature distributions and predictive models.

International Journal of Innovative Research of Science, Engineering and Technology (IJIRSET)

Impact Factor 9.935

|www.ijirset.com |A Monthly, Peer Reviewed & Refereed Journal| e-ISSN: 2319-8753| p-ISSN: 2347-6710|

Volume 15, Issue 11, November 2026

|DOI: 10.15680/IJIRSET.2026.1511028|

TABLE 1: Classification results for Comparison of features and models

Feature set	LightGBM			CNN			KNN			SVM		
	Acc	Prec	F1	Acc	Prec	F1	Acc	Prec	F1	Acc	Prec	F1
Mean & std	**86.24**	**84.12**	**84.15**	51.57	50.23	50.25	82.00	81.66	81.73	55.98	55.06	55.11
Frequency bands	63.18	67.56	67.63	32.70	33.39	33.42	70.00	72.14	72.21	35.06	37.56	37.62
Mean & std + bands	84.34	83.82	83.86	52.02	51.67	51.75	81.00	80.53	80.61	52.36	50.98	51.06

The comparative statistical analysis reveals that the simplified time-domain features (mean and standard deviation) consistently yielded the highest classification accuracy. The foundational statistical feature set ("Mean & std") demonstrated the highest predictive accuracy (86.24%) when fitted with the LightGBM ensemble algorithm. The LightGBM ensemble demonstrated high predictive stability across the 5-fold cross-validation, yielding a low standard deviation of variance. Conversely, the "Frequency bands" feature set yielded the highest statistical error and lowest mean accuracy across all evaluated models.

The deep learning (CNN) and maximum-margin (SVM) architectures exhibited poor convergence and significantly lower performance compared to the ensemble (LightGBM) and non-parametric (KNN) approaches. The combined feature space ("Mean & std + bands") produced competitive results, but failed to surpass the predictive power of the pure statistical moments for the primary classifiers, confirming the sufficiency of lower-dimensional statistical features.

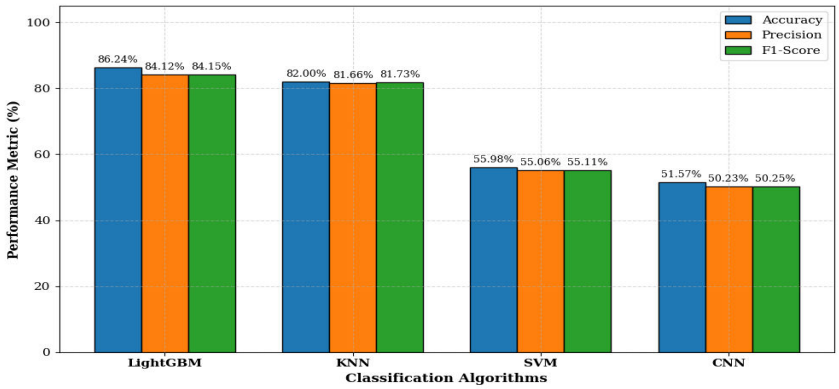

Fig. 7: Comparative statistical performance of machine learning classifiers utilizing time-domain EEG features.

When treating the multi-class problem through a binarized, one-vs-all statistical framework (Table 2), the LightGBM ensemble maintained its superiority, achieving an accuracy of 93.89% for the "Relax vs. all" classification and 86.77% for the "Stress vs. all" classification.

TABLE 3: Classification results of One vs All

	LightGBM			CNN			KNN			SVM		
	Acc	Prec	F1	Acc	Prec	F1	Acc	Prec	F1	Acc	Prec	F1
Stress vs the rest	86.77	86.54	86.67	69.03	67.98	68.05	77.00	78.22	78.27	63.41	61.09	61.13
Relax vs the rest	**93.89**	**93.94**	**93.91**	51.08	50.12	50.20	77.00	77.25	77.25	63.41	61.76	61.76

Beyond predictive accuracy, the computational time complexity of the feature extraction process highlights the efficiency of time-domain statistics (Table 4).

International Journal of Innovative Research of Science, Engineering and Technology (IJIRSET)

Impact Factor 9.935

|www.ijirset.com |A Monthly, Peer Reviewed & Refereed Journal| e-ISSN: 2319-8753| p-ISSN: 2347-6710|

Volume 15, Issue 11, November 2026

|DOI: 10.15680/IJIRSET.2026.1511028|

TABLE 4: Average computational times

Feature set	Time (ms)
Mean & std	**588**
Frequency bands	1,123

Extracting the mean and standard deviation required significantly less computational time (588 ms) compared to the frequency band extraction (1,123 ms), confirming that first-order statistical moments offer a highly optimized approach for dimensionality reduction.

TABLE 5: Classification results of Window size

Feature set	Window size	Acc	Prec	F1
Mean & std	1s	**86.24**	**84.12**	**84.15**
	10s	85.13	86.51	86.53
	20s	83.55	88.90	88.92
Frequency bands	1s	63.18	67.56	67.63
	10s	63.40	69.37	69.47
	20s	65.44	69.59	69.64
Mean & std + bands	1s	84.34	83.82	83.86
	10s	84.20	83.78	83.80
	20s	83.25	81.23	81.22

4.2 Temporal Window Sensitivity Analysis Table 5 illustrates the variance in classification performance as a function of the temporal window size. The "Mean & std" feature set exhibited a slight degradation in statistical accuracy when the sampling window was expanded from 1 second to 10 and 20 seconds. This suggests that smaller temporal windows capture fine-grained variance crucial for this feature set. In contrast, the "Frequency bands" feature set demonstrated a positive correlation with window size, indicating that broader temporal ranges are required to capture stable spectral distributions.

4.3 Intra-Subject Variance and Generalizability Figure 7 illustrates the intrasubject variance in classification accuracy across the individual participants.

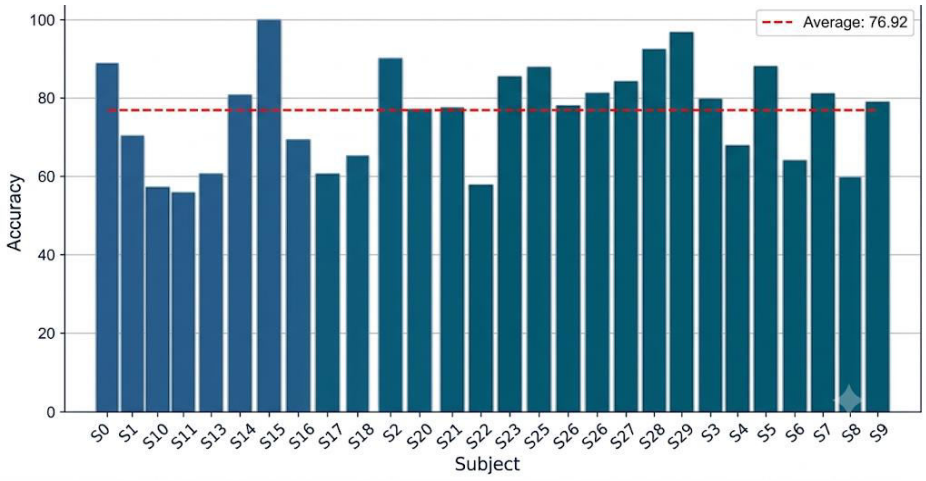

Fig. 8: Intra-subject wise classification results

International Journal of Innovative Research of Science, Engineering and Technology (IJIRSET)

Impact Factor 9.935

|www.ijirset.com |A Monthly, Peer Reviewed & Refereed Journal| e-ISSN: 2319-8753| p-ISSN: 2347-6710|

Volume 15, Issue 11, November 2026

|DOI: 10.15680/IJIRSET.2026.1511028|

While the inter-subject population model achieved an 86.24% accuracy, the intra-subject analysis reveals substantial physiological variability, with individual predictive accuracies fluctuating significantly around a mean of 76.92%. This statistical variance underscores the inherent heterogeneity of individual autonomic responses to stress.

4.4 Multivariate Biosignal Contribution Analysis Table 6 quantifies the statistical contribution of integrating multiple physiological modalities.

TABLE 6: Comparison between EEG and ECG + EDA data

Biosignals	Acc	Prec	F1
EEG	85.13	86.51	86.53
ECG + EDA	75.88	75.46	75.04
EEG + ECG + EDA	**91.44**	**91.54**	**91.42**

Models fitted exclusively on EEG data outperformed models fitted on the combined ECG and EDA data by over 10 percentage points. However, a multivariate approach integrating all three biosignals (EEG, ECG, and EDA) maximized the classification accuracy to 91.44%.



Fig. 9: Impact of multivariate biosignal integration on classification accuracy, comparing isolated peripheral signals (ECG + EDA), isolated neural signals (EEG), and the combined multimodal framework.

This discriminative power is further validated by the Receiver Operating Characteristic (ROC) curve analysis.

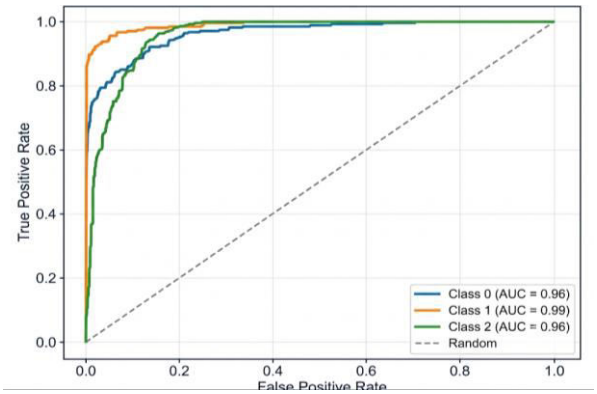

Fig. 10: ROC Curve: EEG (0: relax, 1: neutral, 2: stress)

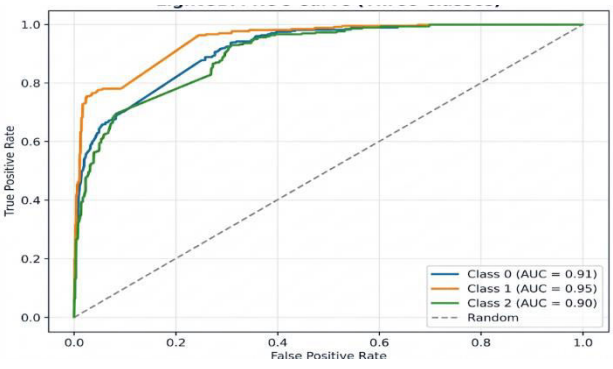

Fig. 11: ROC Curve: ECG + EDA (0: relax, 1: neutral, 2: stress)

International Journal of Innovative Research of Science, Engineering and Technology (IJIRSET)

Impact Factor 9.935

|www.ijirset.com |A Monthly, Peer Reviewed & Refereed Journal| e-ISSN: 2319-8753| p-ISSN: 2347-6710|

Volume 15, Issue 11, November 2026

|DOI: 10.15680/IJIRSET.2026.1511028|

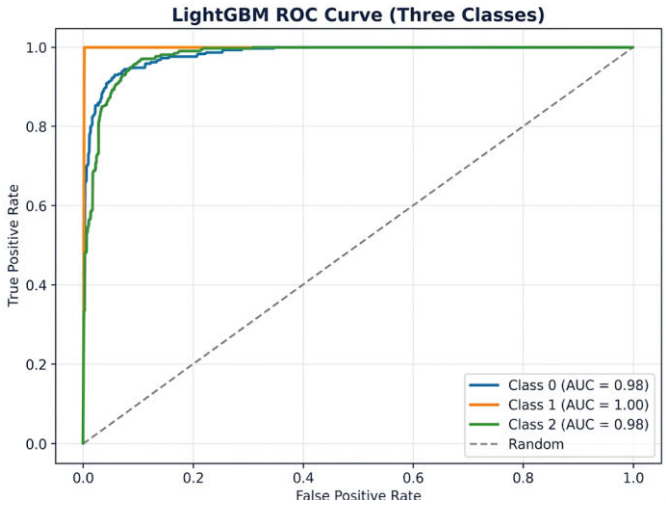

Fig. 12: ROC Curve of EEG + ECG + EDA (0: relax, 1: neutral, 2: stress)

The isolated EEG classifier (Fig. 8) demonstrated robust Area Under the Curve (AUC) metrics (0.96 for Class 0, 0.99 for Class 1, and 0.96 for Class 2). While the isolated ECG + EDA classifier (Fig. 9) also showed strong discriminative capability, the fully integrated multivariate model (Fig. 10) achieved near-perfect AUC values of 0.98, 1.00, and 0.98, demonstrating the synergistic statistical benefits of high-dimensional, multimodal data integration.

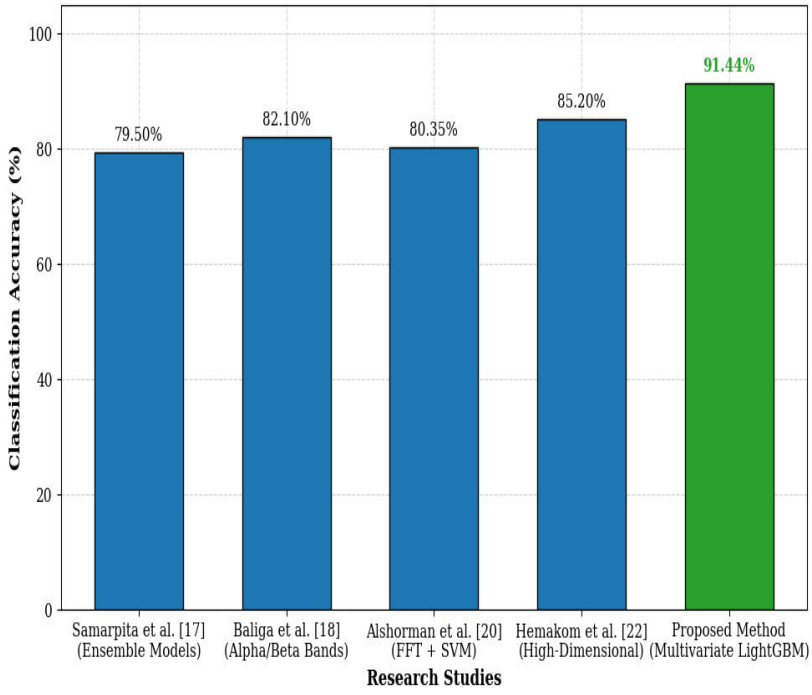

Fig. 13: Predictive performance benchmark of the proposed multivariate LightGBM framework against existing frequency-domain, ensemble, and high-dimensional classification methodologies in the literature.

4.5 Spatial Variance and Electrode Importance To determine which spatial features contribute the most significant variance to the predictive model, a split-and-gain feature importance analysis was conducted on the EEG channels.

International Journal of Innovative Research of Science, Engineering and Technology (IJIRSET)

Impact Factor 9.935

|www.ijirset.com |A Monthly, Peer Reviewed & Refereed Journal| e-ISSN: 2319-8753| p-ISSN: 2347-6710|

Volume 15, Issue 11, November 2026

|DOI: 10.15680/IJIRSET.2026.1511028|

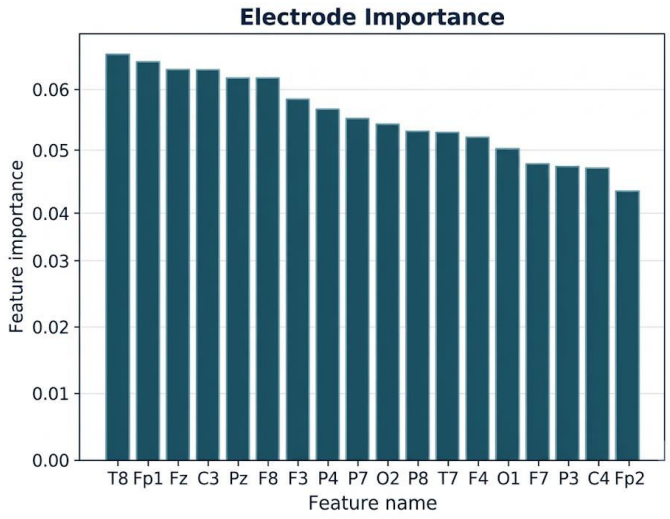

Fig. 14: All three signals Electrode Importance

The analysis revealed that the temporal electrode "T8" held the highest statistical importance (0.065643), closely followed by the frontal and central electrodes "Fp1" (0.064449), "Fz" (0.063147), and "C3" (0.063115). Conversely, occipital and parietal electrodes such as "O1", "P3", and "C4" contributed the least variance to the model's decision boundaries.

V. DISCUSSION

The statistical evaluation demonstrates that EEG time-series data captures highly significant variance for the objective classification of stress states, a finding consistent with emerging biostatistical literature. When comparing single-modality models, cardiovascular and electrodermal data (ECG and EDA) exhibited a 12.19% higher predictive error rate compared to isolated EEG data. Integrating all three biometric variables into a fully multivariate model maximized classification accuracy (yielding a 7.41% improvement over EEG alone); however, this multi-sensor approach increases instrumentation complexity. The selection of variables in practical applications should therefore balance predictive accuracy against the physical constraints of the monitoring environment.

Methodologically, this study utilized both inter-subject and intra-subject statistical designs. The inter-subject framework ensured that the model's decision boundaries generalized across a diverse population sample, while the intra-subject analysis highlighted the inherent physiological variance and individualized autonomic reactions to the stress protocol. Furthermore, analyzing first-order statistical moments (mean and standard deviation) drastically reduced computational overhead compared to high-dimensional transformations, proving that complex feature spaces are not strictly necessary for robust predictive modeling. The spatial variance analysis confirmed that specific localized electrodes contribute the most statistically significant data, which holds profound implications for reducing the dimensionality and physical footprint of future wearable biometric sensors.

VI. CONCLUSION AND FUTURE SCOPE

The empirical modeling of physiological signals has gathered significant interest for its potential to replace subjective psychological evaluations with objective, quantifiable metrics. This study presented a comprehensive statistical evaluation of continuous EEG, EDA, and ECG time-series data to classify discrete stress states. The results confirm that foundational time-domain statistical features (mean and standard deviation), when paired with an optimized gradient-boosting ensemble (LightGBM), minimize classification error more effectively than computationally heavy algorithms or complex frequency transformations. While EEG data independently provides the highest discriminative variance, a fully multivariate integration of all physiological signals yields the optimal predictive outcome.

International Journal of Innovative Research of Science, Engineering and Technology (IJIRSET)

Impact Factor 9.935

|www.ijirset.com |A Monthly, Peer Reviewed & Refereed Journal| e-ISSN: 2319-8753| p-ISSN: 2347-6710|

Volume 15, Issue 11, November 2026

|DOI: 10.15680/IJIRSET.2026.1511028|

Future biostatistical research should focus on longitudinal modeling to incorporate contextual and environmental covariates into the stress detection framework. Furthermore, investigating probabilistic attention mechanisms to dynamically weight feature variance in real-time could further optimize the predictive accuracy of these models in applied settings.

REFERENCES

1. World Health Organization. (2023, February 21). Questions and answers on stress. Retrieved from https://www.who.int/news-room/questions-and-answers/item/stress (accessed on March 26, 2024).
2. D. Lecic-Tosevski, O. Vukovic and J. Stepanovic, "Stress and personality," Psychiatrike = Psychiatriki, 22(4), 290–297, 2011.
3. P. E. Flores-Kanter, L. Moretti, and L. A. Medrano, "A narrative review of emotion regulation process in stress and recovery phases," Heliyon, vol. 7, no. 6, Jun. 2021, p. e07218, doi: 10.1016/j.heliyon.2021.e07218.
4. A.D. Crosswell, K.G. Lockwood, "Best practices for stress measurement: How to measure psychological stress in health research," Health Psychol Open, 2020, doi: 10.1177/2055102920933072.
5. R. Martínez, E. Irigoyen, A. Arruti, J.I. Martin and J. Muguerza, "A Real-Time Stress Classification System based on Arousal Analysis of the Nervous System by an F-State Machine," Computer Methods and Programs in Biomedicine, vol. 148, 2017.
6. R. Nawaz, K. H. Cheah, H. Nisar and V. V. Yap, "Comparison of different feature extraction methods for EEG-based emotion recognition," Biocybern. Biomed. Eng., vol. 40, no. 3, pp. 910–926, 2020.
7. F. Agrafioti, D. Hatzinakos and A. K. Anderson, "ECG pattern analysis for emotion detection," IEEE Trans. Affective Comput., vol. 3, no. 1, pp. 102–115, First Quarter 2012.
8. R. Martinez, A. Salazar-Ramirez, A. Arruti, E. Irigoyen, J. I. Martin and J. Muguerza, "A Self-Paced Relaxation Response Detection System Based on Galvanic Skin Response Analysis," in IEEE Access, vol. 7, pp. 43730-43741, 2019.
9. Y. Shan, S. Li and T. Chen, "Respiratory signal and human stress: non-contact detection of stress with a low-cost depth sensing camera," International Journal of Machine Learning and Cybernetics, 2020, doi: 10.1007/s13042-020-01074-x.
10. S. A. Patil and A. N. Paithane, "Comprehensive Review of EEGBased Algorithms for Mental Stress Analysis," IEEE International Conference on Computational Intelligence and Ubiquitous Computing for Biomedical Applications (CIBEC), 2023, pp. 1-7, doi: 10.1109/ICCUBEA58933.2023.10392207.
11. M.B. Bin Heyat, F. Akhtar, S.J. Abbas, M. Al-Sarem, A. Alqarafi, A. Stalin, R. Abbasi, A.Y. Muaad, D. Lai and K. Wu, "Wearable Flexible Electronics Based Cardiac Electrode for Researcher Mental Stress Detection System Using Machine Learning Models on Single Lead Electrocardiogram Signal," Biosensors, 2022, 12, 427. https://doi.org/10.3390/bios12060427.
12. E. Hosseini et al., "A Low Cost EDA-based Stress Detection Using Machine Learning," 2022 IEEE International Conference on Bioinformatics and Biomedicine (BIBM), Las Vegas, NV, USA, 2022, pp. 2619-2623, doi: 10.1109/BIBM55620.2022.9995093.
13. Asif, M. Majid and S. M. Anwar, "Human stress classification using EEG signals in response to music tracks," Comput. Biol. Med., vol. 107, pp. 182-196, 2019.
14. G. Avila, F. S. Bott, L. Tiemann, V. D. Hohn, E. S. May, M. M. Nickel, P. T. Zebhauser, J. Gross, and M. Ploner, "DISCOVER-EEG: an open, fully automated EEG pipeline for biomarker discovery in clinical neuroscience," Scientific Data, vol. 10, no. 1, Sep. 2023, p. 613, doi: 10.1038/s41597-023-02525-0.
15. Gosala, P. D. Kapgate, P. Jain, R. N. Chaurasia, and M. Gupta, "Wavelet transforms for feature engineering in EEG data processing: An application on Schizophrenia," Biomedical Signal Processing and Control, vol. 85, Aug. 2023, p. 104811, doi: 10.1016/J.BSPC.2023.104811.
16. N. Armanfard, M. Komeili, J. P. Reilly, and L. Pino, "Vigilance lapse identification using sparse EEG electrode arrays," Canadian Conference on Electrical and Computer Engineering (CCECE), Oct. 2016, doi: 10.1109/CCECE.2016.7726846.
17. S. Samarpita, R. Satpathy, B. Mishra and R. Mishra, "Differentiating Mental Stress Levels: Analysing Machine Learning Algorithms Comparatively For EEG-Based Mental Stress Classification Using MNE-Python," Journal of Advanced Zoology, 2023, doi: 10.17762/jaz.v44iS5.2013.
18. S. Baliga, N. Ali, A. LS and V. P, "Emotion Recognition and Stress Reduction Based on Electroencephalograph (EEG) Signals validated by Machine Learning Algorithms," 2023 International Conference on Smart Systems for

International Journal of Innovative Research of Science, Engineering and Technology (IJIRSET)

Impact Factor 9.935

|www.ijirset.com |A Monthly, Peer Reviewed & Refereed Journal| e-ISSN: 2319-8753| p-ISSN: 2347-6710|

Volume 15, Issue 11, November 2026

|DOI: 10.15680/IJIRSET.2026.1511028|

applications in Electrical Sciences (ICSSES), Tumakuru, India, 2023, pp. 1-6, doi: 10.1109/ICSSES58299.2023.10199291.

19. A.J. Marthinsen, I.T. Galtung1, A. Cheema1, C.M. Sletten1, I.M. Andreassen1, Øystein Sletta1, A. Soler1 and M. Molinas, "Psychological stress detection with optimally selected EEG channel using Machine Learning techniques," CEUR Workshop Proceedings, 2023, 53-68.
20. O. AlShorman, M. Masadeh, Md B.B. Heyat, F. Akhtar, H. Almahasneh, G. Md Ashraf and A. Alexiou, "Frontal lobe real-time EEG analysis using machine learning techniques for mental stress detection," J. Integr. Neurosci., 2022, 21(1), 20.
21. Nirabi, F. A. Rahman, M. H. Habaebi, K. A. Sidek and S. Yusoff, "Machine Learning-Based Stress Level Detection from EEG Signals," 2021 IEEE 7th International Conference on Smart Instrumentation, Measurement and Applications (ICSIMA), Bandung, Indonesia, 2021, pp. 53-58, doi: 10.1109/ICSIMA50015.2021.9526333.
22. Hemakom, D. Atiwiwat and P. Israsena, "ECG and EEG based detection and multilevel classification of stress using machine learning for specified genders: A preliminary study," PLoS One, 2023 Sep 1;18(9):e0291070. doi: 10.1371/journal.pone.0291070.
23. P. Zontone, A. Affanni, R. Bernardini, A. Piras and R. Rinaldo, "Stress Detection Through Electrodermal Activity (EDA) and Electrocardiogram (ECG) Analysis in Car Drivers," 2019 27th European Signal Processing Conference (EUSIPCO), A Coruna, Spain, 2019, pp. 1-5, doi: 10.23919/EUSIPCO.2019.8902631.
24. Affani, "Wireless Sensors System for Stress Detection by Means of ECG and EDA Acquisition," Sensors, vol. 20, no. 7, 2020, doi: 10.3390/s20072026.
25. T. Umematsu, A. Sano, S. Taylor and R. W. Picard, "Improving Students' Daily Life Stress Forecasting using LSTM Neural Networks," 2019 IEEE EMBS International Conference on Biomedical & Health Informatics (BHI), Chicago, IL, USA, 2019, pp. 1-4, doi: 10.1109/BHI.2019.8834624.
26. P. Bobade and M. Vani, "Stress Detection with Machine Learning and Deep Learning using Multimodal Physiological Data," 2020 Second International Conference on Inventive Research in Computing Applications (ICIRCA), Coimbatore, India, 2020, pp. 51-57.
27. J. Shin, J. Maeng and D.-H. Kim, "Inner emotion recognition using multi bio-signals," in Proc. IEEE Int. Conf. Consum. Electron.-Asia, 2018, pp. 206–212.
28. M. Norden, AG Hofmann, M. Meier, F. Balzer, OT Wolf, E. Bottinger and H. Drimalla, "Inducing and Recording Acute Stress Responses on a Large Scale With the Digital Stress Test (DST): Development and Evaluation Study," J Med Internet Res, 2022, doi: 10.2196/32280.
29. M.A. Almazrouei, R.M. Morgan and I.E. Dror, "A method to induce stress in human subjects in online research environments," Behav Res 55, 2023, doi: 10.3758/s13428-022-01915-3.
30. M. Klug and K. Gramann, "Identifying key factors for improving ICA-based decomposition of EEG data in mobile and stationary experiments," The European journal of neuroscience, vol. 54, 2021.
31. L. Sun, Y. Liu and P. J. Beadle, "Independent component analysis of EEG signals," Proceedings of 2005 IEEE International Workshop on VLSI Design and Video Technology, pp. 219-222, 2005.
32. F. Perrin, J. Pernier, O. Bertrand and J. F. Echallier, "Spherical splines for scalp potential and current density mapping," Electroencephalography and Clinical Neurophysiology, vol. 72, Issue 2, 1989.
33. Beste, A. Munchau and C. Frings, "Towards a systematization of brain oscillatory activity in actions," Communications Biology, 6(1), pp. 1–11, 2023, doi: 10.1038/s42003-023-04531-9.
34. E. Perez-Valero, M. Lopez-Gordo and M. Vaquero-Blasco, "EEGbased multi-level stress classification with and without smoothing filter," Biomedical Signal Processing and Control, vol. 69, 2021, doi: 10.1016/j.bspc.2021.102881.
35. M. A. Hafeez and S. Shakil, "EEG-based stress identification and classification using deep learning," Multimedia Tools and Applications, vol. 83, pp. 1-17, 2023, doi: 10.1007/s11042-023-17111-0.
36. H. Bian, Y. Bian, J. Li, S. Xu, X. Shao, J. Li and B. Jiang, "A simple hand mnemonic for teaching the cardiac cycle," Advances in Physiology Education, vol. 44, no. 1, 2019.
37. de Santos Sierra, C. S. Avila, J. G. Casanova, and G. B. del Pozo, "A stress-detection system based on physiological signals and fuzzy logic," IEEE Trans. Ind. Electron., vol. 58, no. 10, pp. 4857–4865, Oct. 2011, doi: 10.1109/TIE.2010.2103538.
38. J. A. Healey and R. W. Picard, "Detecting stress during real-world driving tasks using physiological sensors," IEEE Trans. Intell. Transp. Syst., vol. 6, no. 2, pp. 156–166, Jun. 2005.
39. H. F. Posada-Quintero, J. P. Florian, A. D. Orjuela-Canon and K. H. Chon, "Electrodermal Activity Is Sensitive to Cognitive Stress under Water," Front Physiol., 2018, Jan 17; 8:1128, doi: 10.3389/fphys.2017.01128.

International Journal of Innovative Research of Science, Engineering and Technology (IJIRSET)

Impact Factor 9.935

|www.ijirset.com |A Monthly, Peer Reviewed & Refereed Journal| e-ISSN: 2319-8753| p-ISSN: 2347-6710|

Volume 15, Issue 11, November 2026

|DOI: 10.15680/IJIRSET.2026.1511028|

40. TM. Bynion, M.T. Feldner, ”Self-Assessment Manikin,” Encyclopedia of Personality and Individual Differences, Springer, 2017, doi: 10.1007/978-3-319-28099-8 77-1.
41. H. Ali, M. Salleh, K. Hussain, A. Ullah, A. Ahmad and R. Naseem, ”A review on data preprocessing methods for class imbalance problem,” International Journal of Engineering & Technology, 390-397, 2019, doi: 10.14419/ijet.v8i3.29508.
42. N. V. Chawla, K. W. Bowyer, L. O. Hall and W. P. Kegelmeyer, ”SMOTE: synthetic minority over-sampling technique,” J. Artif. Int. Res., vol. 16, 2002, 321–357.
43. H. Zeng, C. Yang, H. Zhang, W. Zhenhua, J. Zhang, G. Dai, F. Babiloni and W. Kong, ”A LightGBM-Based EEG Analysis Method for Driver Mental States Classification,” Computational Intelligence and Neuroscience, 2019. 1-11. 10.1155/2019/3761203.
44. S. Aggarwal, L. Aggarwal, M. S. Rihal and S. Aggarwal, ”EEG Based Participant Independent Emotion Classification using Gradient Boosting Machines,” 2018 IEEE 8th International Advance Computing Conference (IACC), Greater Noida, India, 2018, pp. 266-271, doi: 10.1109/IADCC.2018.8692106.
45. Acharya et al., ”Multi-class Emotion Classification Using EEG Signals,” Communications in Computer and Information Science, vol. 1367. Springer, IACC 2020.
46. Q. Que and M. Belkin, ”Back to the Future: Radial Basis Function Network Revisited,” in IEEE Transactions on Pattern Analysis and Machine Intelligence, vol. 42, no. 8, pp. 1856-1867, 1 Aug. 2020, doi: 10.1109/TPAMI.2019.2906594.
47. H. Frohlich et al., ”From hype to reality: data science enabling personalized medicine,” BMC Med., 2018, doi: 10.1186/s12916-0181122-7.
48. T. Iqbal, A.J. Simpkin, D. Roshan, N. Glynn, J. Killilea, J. Walsh, G. Molloy, S. Ganly, H. Ryman, E. Coen et al. ”Stress Monitoring Using Wearable Sensors: A Pilot Study and Stress-Predict Dataset,” Sensors, 2022, doi: 10.3390/s22218135.
49. S. Liu, Z. Wang, Y. An, J. Zhao, Y. Zhao and Y. Zhang, ”EEG emotion recognition based on the attention mechanism and pretrained convolution capsule network,” Knowledge-Based Systems, vol. 265, 2023.



ISSN INTERNATIONAL STANDARD SERIAL NUMBER INDIA

INNO SPACE SJIF Scientific Journal Impact Factor

doi crossref

निस्केयर NISCAIR

INTERNATIONAL JOURNAL OF INNOVATIVE RESEARCH

IN SCIENCE | ENGINEERING | TECHNOLOGY

9940 572 462 6381 907 438 ijirset@gmail.com

www.ijirset.com

Scan to save the contact details